Title: Prediction of smoke filling in large volumes by means of data assimilation-based numerical simulations

Authors: Tarek Beji, Steven Verstockt, Rik Van de Walle, Bart Merci

In: Journal of Fire Sciences, Volume 30, issue 4, pages 300-317

Optional: http://dx.doi.org/10.1177/0734904112437845

Title: Prediction of smoke filling in large volumes by means of data assimilation based numerical simulations

Author names and affiliations: Tarek Beji[a], Steven Verstockt[b], Rik Van de Walle[b], Bart Merci[a]

[a] Ghent University – UGent, Dept. Flow, Heat and Combustion Mechanics, Sint-Pietersnieuwstraat 41, B-9000 Ghent, Belgium

[b] Dept. Electronics and Information Systems, Multimedia Lab, Ghent University – IBBT, Gaston Crommenlaan 8, Bus 201, B-9050 Ledeberg-Ghent, Belgium

E-mail addresses of the authors:

1. Tarek Beji: Tarek.Beji@UGent.be

2. Steven Verstockt: Steven.Verstockt@UGent.be

3. Rik Van de Walle: rik.vandewalle@UGent.be

4. Bart Merci: Bart.Merci@UGent.be

Corresponding author:

Dr. Tarek Beji

Ghent University – Ugent, Department of Flow, Heat and Combustion Mechanics, St. Pietersnieuwstraat 41

Tel : ++32 9 264 98 46; Fax : ++32 9 264 35 75

E-mail: Tarek.Beji@UGent.be

Biography of Tarek Beji (corresponding author)

Tarek Beji is a postdoctoral researcher at the University of Ghent (Belgium) in the group of Pr. Bart Merci. He received his PhD from the University of Ulster (United Kingdom) in Fire Engineering in 2009. Since 2006 he has been working in the areas of enclosure fires and soot modelling.

Prediction of smoke filling in large volumes by means of data assimilation based numerical simulations

ABSTRACT

The concept of numerical simulations for real-time Numerical Fire Forecasting (NFF) is illustrated for the case of natural smoke filling of a large scale atrium in case of fire. The numerical simulations are performed within the Inverse Zone Modelling framework. The technique consists of assimilating collected data for a certain parameter, *in casu* the smoke layer height, into the zone model in order to estimate an unknown of the problem ('model invariant', MI), mainly the fire heat release rate. A forecast in terms of evolution of smoke level and temperature can then be produced. Because zone model calculations are very fast, positive lead times of several minutes are obtained. The developed model produces reliable forecasts for the cases considered. Equally important, the robustness of the technique is illustrated: the sensitivity of the results to the 'initial guess' of the MI(s) is small (i.e., the method converges easily); one MI is sufficient to obtain reliable predictions for smoke layer height evolution; the data assimilation window length does not affect the results significantly. The method automatically provides a different value for the plume entrainment constant, depending on the position of the fire (in the middle of the atrium or in a corner).

KEYWORDS

Numerical Fire Forecast (NFF), Data Assimilation (DA), inverse modeling, Tangent Linear Model (TLM), two-zone model, smoke filling

INTRODUCTION

Producing a real-time 'Numerical Fire Forecast' (NFF) is one of the recent great challenges in the fire community today. Predicting fire evolution with a sufficiently large positive lead time can assist a decision support system and guide intervention strategies, as first illustrated in the 'FireGrid' project [1]. The main idea consists of performing a continuous dynamic estimation of the fire evolution by incorporating live data from sensor readings [2]. This enables the display of future hazards in terms of smoke levels, structural collapse and flashover occurrence. Evacuation and fire service interventions can then be facilitated and/or adjusted 'on the go'. Different aspects of the problem need to be tackled, e.g. sensing, modeling and forecasting. Recent developments on the sensing part, e.g. the use of video to provide information on flames and smoke [3-8], are not described here. Rather, we focus on the modeling and forecast parts. The technique applied is the Inverse Zone Modelling technique in conjunction with Data Assimilation (DA) [9-10]. The DA technique has already been used extensively in Numerical Weather Predictions (NWP). It consists of incorporating information from 'observed data' into an 'assimilating model'. An 'analysis' is performed, based on which a forecast is produced that matches best the 'observed state'. This forecast gives in real time a display of future developments [11]. The 'lead' time of the forecast is determined by a certain accuracy (or reliability) criterion. Obviously, the computational time must be short enough, compared to this lead time, in order to generate a prediction, ahead of the event. Although theoretical work is undertaken to apply DA to the fundamental Navier-Stokes equations [12], which are solved in Computational Fluid Dynamics (CFD), Zone Modelling is a much better option from a computational point of view to predict the fire development in its early stages. Indeed, computing times are orders of magnitude smaller and the 'loss' of physics in a Zone Model compared to CFD is compensated, using the contribution of DA by the dynamic adjustment of model parameters.

As mentioned in [1], "*the data assimilation philosophy needs to be subjected to great scrutiny prior to exploitation in fire applications*". The approach, carefully described in [9-10], is adopted here. For the scenario considered in this paper, we examine in detail the potential to predict the natural smoke filling process of an atrium due to a fire without prior knowledge of the fire location, size or heat release rate (HRR). This is a basic development step, prior to the prediction of fire development itself. The data used for assimilation stems from experiments [13], where the fire is constant in size and HRR. In addition to the illustration that reliable forecasts are obtained, including automatic 'determination' of the fire location, the following aspects are addressed in a sensitivity study:

- impact of addition of a second MI;
- impact of initial guess for MI(s) on the convergence of the optimization process;
- impact of the DA window (length and timing).

To the best of the authors' knowledge, it is the first time that DA based numerical simulations are applied to forecasting of smoke filling in case of fire, including such a sensitivity study.

EXPERIMENTAL CONFIGURATION

The numerical calculations are based on a series of fire tests conducted in a full-scale facility at The PolyU/USTC atrium located at the State Key Laboratory of Fire Science of University of Science and Technology of China [13, 14]. This atrium, constructed for experimental studies on smoke movement, has inner dimensions of 22.4 m × 11.9 m and 27 m ceiling height. The dimensions of the two side doors are 4 m × 2 m (Fig. 1). The fire is generated by means of an oil burner. The oil flow rate is defined at the surface to produce the specified fire intensity. In the cases considered in this work, the fire source is 2 m x 2 m with HRR per unit area of 1000 kW/m^2, generating therefore a total fire HRR of 4000 kW. Two different locations of the fire are

considered: in the center (Case A) and in the corner (Case C) of the atrium floor. The measurements include the smoke layer height and average temperature.

For the sake of simplicity, the calculations performed here are made only for the natural filling cases. Natural and/or mechanical venting is not considered, although the method can deal with ventilation as well. The experimental data used in the present paper is shown in Fig. 2.

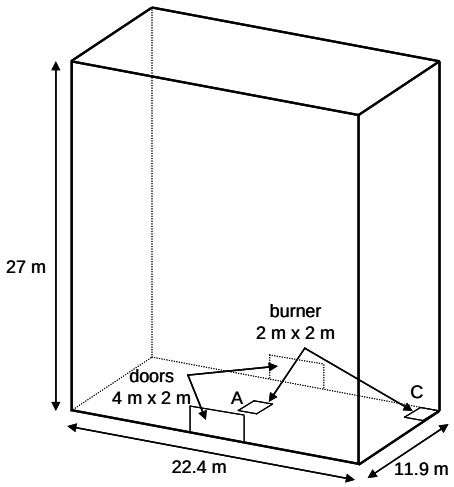

Figure 1. Schematic representation of the geometry [13]. Shafts, fans and windows for mechanical and natural ventilation are not represented.

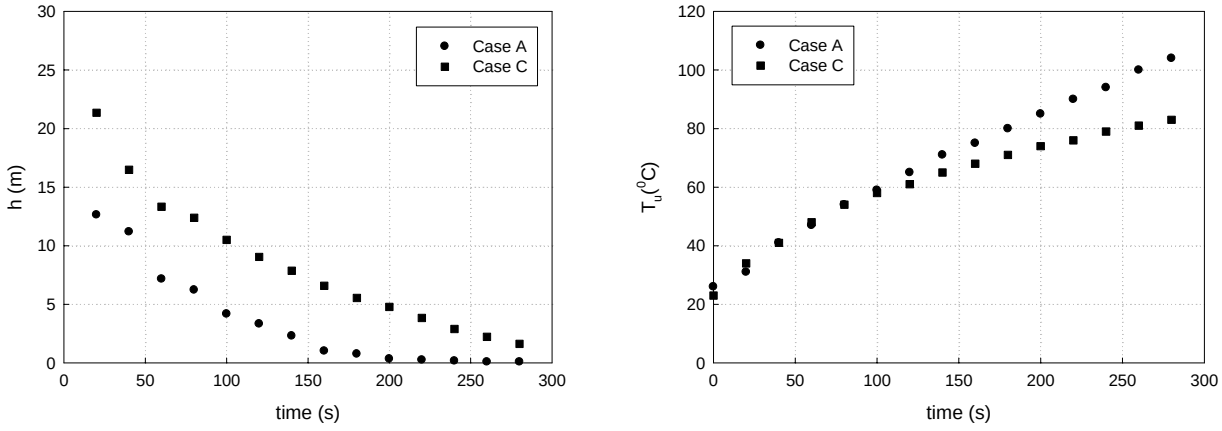

Figure 2. Experimental data (every 20 s) for smoke filling in an atrium [13]. Smoke layer height (left) and mean smoke layer temperature (right) for two fire locations (centre, case A, and corner, case C).

MODEL FORMULATION

Zone Model

Although less sophisticated than CFD, zone modeling has the important advantage of being much less time consuming. This is essential in the application at hand, since forecasts must be obtained sufficiently fast. Results from zone models are obtained practically instantaneously, since the problem formulation is reduced to the basic conservation equations for mass and energy, applied to only 2 zones (hot upper layer and cold lower layer). Compared to detailed CFD, there is a 'loss' of correct physics in the sub-models, particularly plume entrainment in the cases at hand. This can be largely overcome by continuously updating model parameters in a dynamical system, through data assimilation, as explained below. It will, e.g., be illustrated that the method as presented automatically 'determines' whether the fire source is in a corner or not.

Although the conservation equations for mass and energy for the upper layer are well-known, they are briefly repeated here for the case of natural filling (*i.e.* no natural or mechanical venting):

$$\frac{d\left(\rho_u V_u\right)}{dt} = \dot{m}_p \ , \quad \frac{dE}{dt} = \alpha Q_c \tag{1}$$

where ρ_u, V_u, and E are respectively the density, the volume and the energy level of the upper layer. The variable t denotes the time, $\dot{m}_p$ the smoke mass flow rate as it enters the upper layer through the plume and Q_c the convective heat release rate of the fire. α is a coefficient which accounts for heat losses from the upper layer to the environment.

The smoke mass flow rate can be described by several calculations, e.g. [15 - 17]. Here, we deliberately choose the simple expression from [15]:

$$\dot{m}_p = C \times \left(\frac{\rho_a^2 g}{C_p T_a} \right)^{1/3} \times Q_c^{1/3} \times h^{5/3} \tag{2}$$

where C is the entrainment rate, ρ_a the ambient density, g the gravitational acceleration, C_p the specific heat, T_a the ambient temperature, Q_c the convective heat release rate (expressed in kW) and h the smoke free height (i.e. the height, measured from floor level to the bottom of the smoke layer). The reason for this choice is that (a) parameter(s) can be adjusted, using the DA information, which makes the simple expression (2) sufficiently accurate, as shown below.

Choosing the reference level for energy E equal to zero at ambient temperature T_a, the energy contents in the upper layer is:

$$E = \rho_u V_u C_p \left(T_u - T_a \right) \tag{3}$$

The upper layer volume V_u equals:

$$V_u = A_{atrium} \left(H_0 - h \right) \tag{4}$$

where A_{atrium} is the floor area of the atrium, and H_0 the ceiling height.

The initial conditions are $T_u = T_a$ ($\rho_u = \rho_a$) and $h = H_0$ ($V_u = 0$).

Equations (1) to (4) are discretized in time using a Forward Difference Formula (FDF), implemented in an in-house code:

$$\dot{m}_{p,n} = C \left(\frac{\rho_a^2 g}{C_p T_a} \right)^{1/3} Q_c^{1/3} \, h_n^{5/3} \tag{5a}$$

$$\left(\rho_u V_u \right)_{n+1} = \left(\rho_u V_u \right)_n + \Delta t \, \dot{m}_{p,n} \tag{5b}$$

$$E_{n+1} = E_n + \Delta t \; \alpha Q_c \tag{5c}$$

$$T_{u,n+1} = T_a + \frac{E_{n+1}}{\left(\rho_u V_u \right)_{n+1} C_p} \tag{5d}$$

$$\rho_{u,n+1} = \frac{\rho_a T_a}{T_{u,n+1}} \tag{5e}$$

$$V_{u,n+1} = \frac{(\rho_u V_u)_{n+1}}{\rho_{u,n+1}} \tag{5f}$$

$$h_{n+1} = H_0 - \frac{V_{u,n+1}}{A_{atrium}} \tag{5g}$$

where subscripts n and $n+1$ refer to time and Δt is the time step.

Data Assimilation Model

In Data Assimilation (DA), observed information is incorporated into an assimilating model to produce an accurate image of the true physical state of the system and make a forecast of its evolution in time.

Similarly to [9, 18], the assimilating model in our DA application is the zone model that is also used as 'forward model' (FM) in the predictions. The unknown parameters of the problem are Q_c, C and α. In the basic simulations below, we only consider smoke layer height (measured in [13]) for DA. As a result, two of the three unknowns must be prescribed, while the third unknown becomes a 'model invariant' (MI), e.g. $\theta = [C]$ (fixing Q_c and α) or $\theta = [Q_c]$ (fixing C and α). This MI is then determined through the DA by means of an optimization process as described below. In the sensitivity study, we also examine the potential increase in quality of the predictions if both smoke layer height and temperature are 'observed:

$$\hat{y}_i = \begin{pmatrix} \hat{h}_i \\ \hat{T}_{u,i} \end{pmatrix} \tag{6}$$

where $\hat{y}_i$ is the vector of observations at time t_i. Then there are two MIs (e.g. $\theta = [Q_c, C]$ or $\theta = [\alpha, Q_c]$).

To the vector of observations corresponds a vector (with the same dimensions), y_i, of calculated values by the zone model. The purpose of the calculation process is therefore to find the optimized set of values for the MI(s), minimizing the cost function:

$$J(\theta) = \sum_{i=1}^{N} \left[\hat{y}_i - y_i(\theta)\right]^T W_i \left[\hat{y}_i - y_i(\theta)\right] \tag{7}$$

where N is the number of observations and W_i is a weighting matrix, taken here as identity matrix.

By using a gradient-based method and linearizing the forward model around the initial guess, the equation(s) to be solved become(s) [10]:

$$\theta^{k+1} = \theta^k + \left(A^{-1}\, b\right)^T \tag{8}$$

with $A = \sum_{i=1}^{N} H_i^T W_i H_i$ and $b = \sum_{i=1}^{N} H_i^T W_i \left(\hat{y}_i - M_i\right)$. M_i is the output of the forward model at time t_i and $H_i = \nabla M_i$. For the basic calculations, $y_i = h_i$ and $H_i = \frac{\partial h_i}{\partial \theta}$. If we consider two observed variables, h and T_u, and two MIs to be estimated, e.g. Q_c and C, the term ∇M_i becomes:

$$\nabla M_i = \begin{pmatrix} \frac{\partial h_i}{\partial Q_c} & \frac{\partial h_i}{\partial C} \\ \frac{\partial T_{u,i}}{\partial Q_c} & \frac{\partial T_{u,i}}{\partial C} \end{pmatrix} \tag{9}$$

The derivatives are calculated numerically using the Tangent Linear (TL) technique [19]. Perturbations are introduced to the MI(s) and the observed/assimilated variable(s) in eqs. (5a) – (5g). Model parameters that are kept constant, are not perturbed. The solution of eq. (8) is assumed to be reached when the convergence criterion is met, set as:

$$\left|\theta_i^{k+1} - \theta_i^k\right| \le 0.01\ \theta_i^k \tag{10}.$$

If there is more than one MI, criterion (10) must be met for all MIs.

The iterative optimization process starts, as mentioned, with an initial guess for the MI(s). If the initial guess is 'too far' from the 'true values', the calculations might not converge. We illustrate below that the method is very robust with respect to the initial guess(es).

Structure of the Code

The calculation procedure has been implemented in a FORTRAN in-house code. A flow chart is provided in Fig. 3 (without dynamic estimation of the MI value(s)). After reading the input information, cost function (7) is minimized using the Zone Model subroutine (ZM) and the Tangent Linear Zone Model subroutine (ZM_TL). After convergence has been reached, the forecast is made.

The required program inputs are: the maximum time of simulation, the time step, the height of the enclosure, its floor area, the ambient conditions, the number of observations, the time for the initial observation, the time step between two observations and the values of the observations for the data assimilation. The user must also define, among the model unknowns (Q_c, C and α), the MI(s) and the constants, to which predefined values must be assigned.

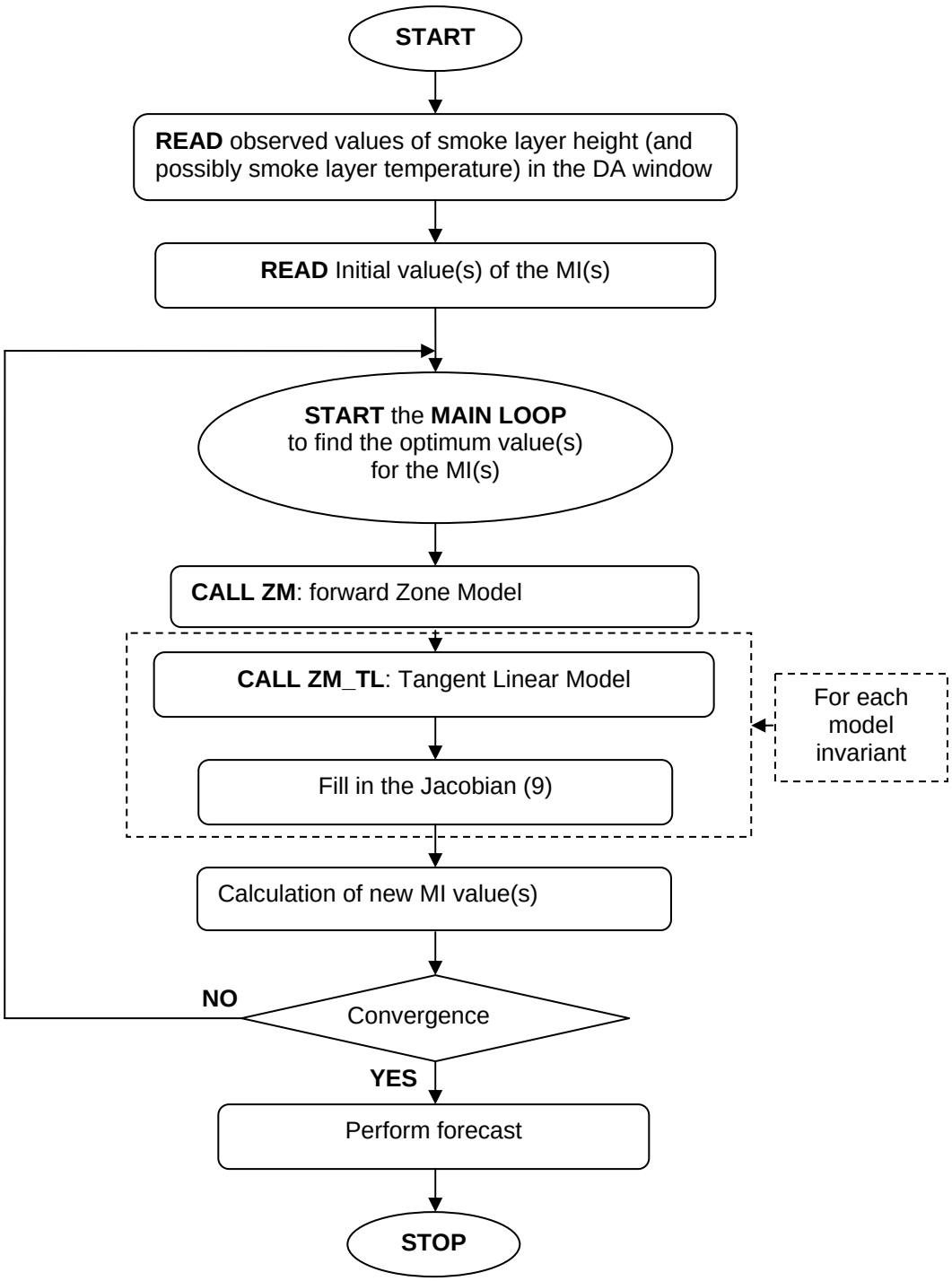

Figure 3. Structure of the code (without dynamic estimation of the MI value(s)).

The program outputs are the optimum value(s) for the MI(s) and the subsequent forecasts of smoke layer height and upper layer temperature. For the time being, the optimization process is performed only once and the forecast is made with steady values for the MI(s). This process can readily be made dynamic, but this is considered beyond the scope of the present paper.

RESULTS AND DISCUSSION

In the discussion of the results, the quality of the forecast is evaluated by calculating the relative deviation, ε, between the prediction and the experimental measurements according to:

$$\varepsilon = \sqrt{\frac{\sum_{i=1}^{n} \left(\hat{\varphi}_i - \varphi_i\right)^2}{\sum_{i=1}^{n} \hat{\varphi}_i^2}} \qquad \textbf{(11)}$$

The variables $\hat{\varphi}_i$ and φ_i denote respectively the experimental measurements and the prediction (i.e. forecast) of h or T_u. The index i varies from 1 to n, which is the number of data points obtained after data assimilation.

Basic Simulations

The basic calculations are performed for the USTC atrium [13] with the fire in the middle, using three data points (*i.e.* N = 3) for smoke layer height h at t = 20 s, 40 s and 60 s (the experimental data was provided every 20 s). Only one MI is chosen then, while the other parameters are kept constant, as summarized in Table 1.

Table 1. Basic simulations: choice of constants and MI.

Case ID	Fire location	Constants	Model Invariant	Assimilation window	Assimilated parameter
USTC_A1	Centre	Q_c = 4000 kW α = 0.6	θ=[C]	N=3, t ∈ [20s, 60s]	h
USTC_A2	Centre	Q_c = 4000 kW C = 0.2	θ=[α]	N=3, t ∈ [20s, 60s]	h
USTC_A3	Centre	α = 0.6 C = 0.2	θ=[Q_c]	N=3, t ∈ [20s, 60s]	h

Table 2 provides the results for the value of the MI as obtained from eq. (8). Clearly, there is some variation in the values. Yet, Figure 4 reveals that hardly any differences are observed in the predictions of smoke layer height. The moment when the smoke reaches the floor (after about 200 s) is well predicted. This implies a positive lead time of more than 2 minutes for the forecasts, regardless of the choice of MI. This illustrates that the method is not very sensitive to the choice of MI. Table 2 reveals a degree of automatic self-regulation in the method, which explains this robustness of the method. Indeed, comparing USTC_A2 to USTC_A1, it is seen that the entrainment coefficient C, prescribed as 0.2 for USTC_A2, is lower than the value obtained in the calculations for USTC_A1 (0.22, see Table 2). This leads to a lower smoke mass flow rate entering the smoke layer (eq. (2)) than in USTC_A1. As such, volume V_u would grow less rapidly, leading to a slower descent of the smoke layer height h. The DA for h then makes sure, though, that this effect due to the lower value for C is compensated by a reduction of the density ρ_u, so that the lower mass flow rate still leads to a comparable volume flow rate. The reduced density is obtained through an increase in temperature T_u. This is achieved by an increase in α (compared to USTC_A1), leading to a more rapid increase in energy level in the upper layer (eq. (1)). A similar reasoning holds for the comparison of USTC_A3 to USTC_A1. Now the fire HRR is higher, compared to USTC_A1, in order to have a sufficiently large volume flow rate. The forecast becomes somewhat less accurate when the fire HRR is the MI, since the HRR determines both the upper layer temperature and the smoke mass flow rate directly.

The forecasts of the upper layer temperature are less accurate. The reason for this is that only one MI is used and the DA is performed on the smoke layer height, not on the temperature. We illustrate below a substantial improvement of the temperature forecast when 2 MIs are used.

Table 2. Basic simulations: value of MI.

Case ID	Constants	MI value
USTC_A1	Q_c = 4000 kW α = 0.6	C = 0.22
USTC_A2	Q_c = 4000 kW C = 0.2	α = 0.77
USTC_A3	α = 0.6 C = 0.2	Q_c = 4730 kW

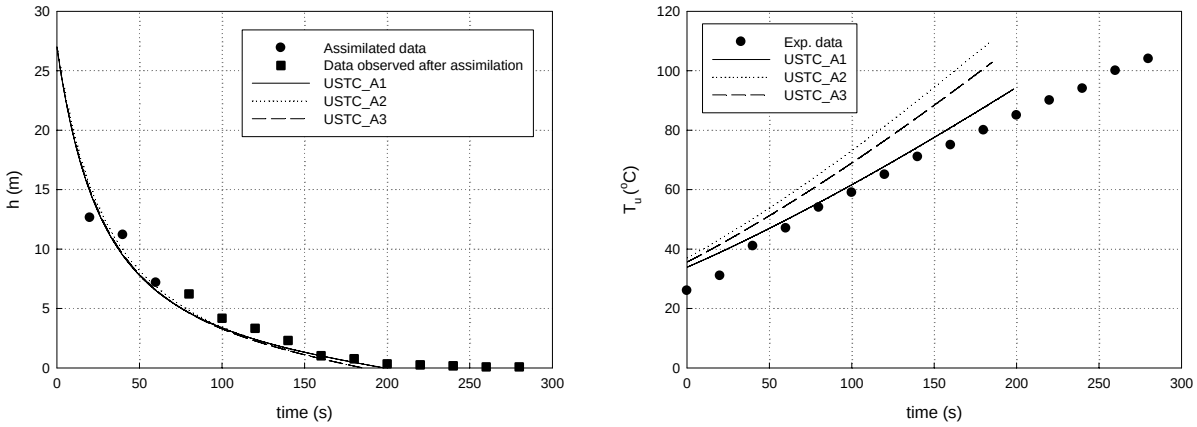

Figure 4. Evolution of smoke layer height (left) and temperature (right) for the fire in the middle of the atrium floor. All symbols refer to experimental data, while lines correspond to simulation results. Only the first three measurements of smoke layer height have been assimilated; temperature data has not been assimilated, it is shown here only for comparison. Legend: see Table 2.

Automatic 'Determination' of Fire Location

In [13], experiments have also been conducted with the fire source placed in the corner of the atrium floor. Obviously, this strongly affects the entrainment of air into the smoke plume. A

general expression for entrainment coefficient C has been developed in [20]: $C = C_m \times k_{LF}^{-2/3}$, in which the entrainment coefficient C_m is taken as constant (C_m = 0.21) and the variable k_{LF} accounts for the fire location (k_{LF} = 1 for axisymmetric plumes, 2 for wall plumes, and 4 for corner plumes). This effectively reduces C from C_m = 0.21 to $0.21 \times 4^{-2/3} = 0.083$ for the corner location. Table 3 illustrates that the values obtained for ASTC_A1 and USTC_1 match these values quite well. The important feature is that this happens 'automatically' in the method, i.e. the different values for C are found by virtue of the DA of the observed valuables during the first minute. Figure 5 reveals a positive lead time in the forecast of 4 minutes, as far as the smoke layer height is concerned, when the fire is positioned in the corner. For USTC_A1, predictions match the experimental data within 26 % for the smoke layer height and 4 % for the upper layer temperature. For USTC_C1, the relative deviation is 15 % for h and 44 % for T_u. The quality of the temperature predictions improves substantially when 2 MIs are used, as shown below.

Table 3. Value of entrainment coefficient for fire in the centre (A) and in the corner (C).

Case ID	Constants	MI value
USTC_A1	Q_c = 4000 kW α = 0.6	C = 0.22
USTC_C1	Q_c = 4000 kW α = 0.6	C = 0.08

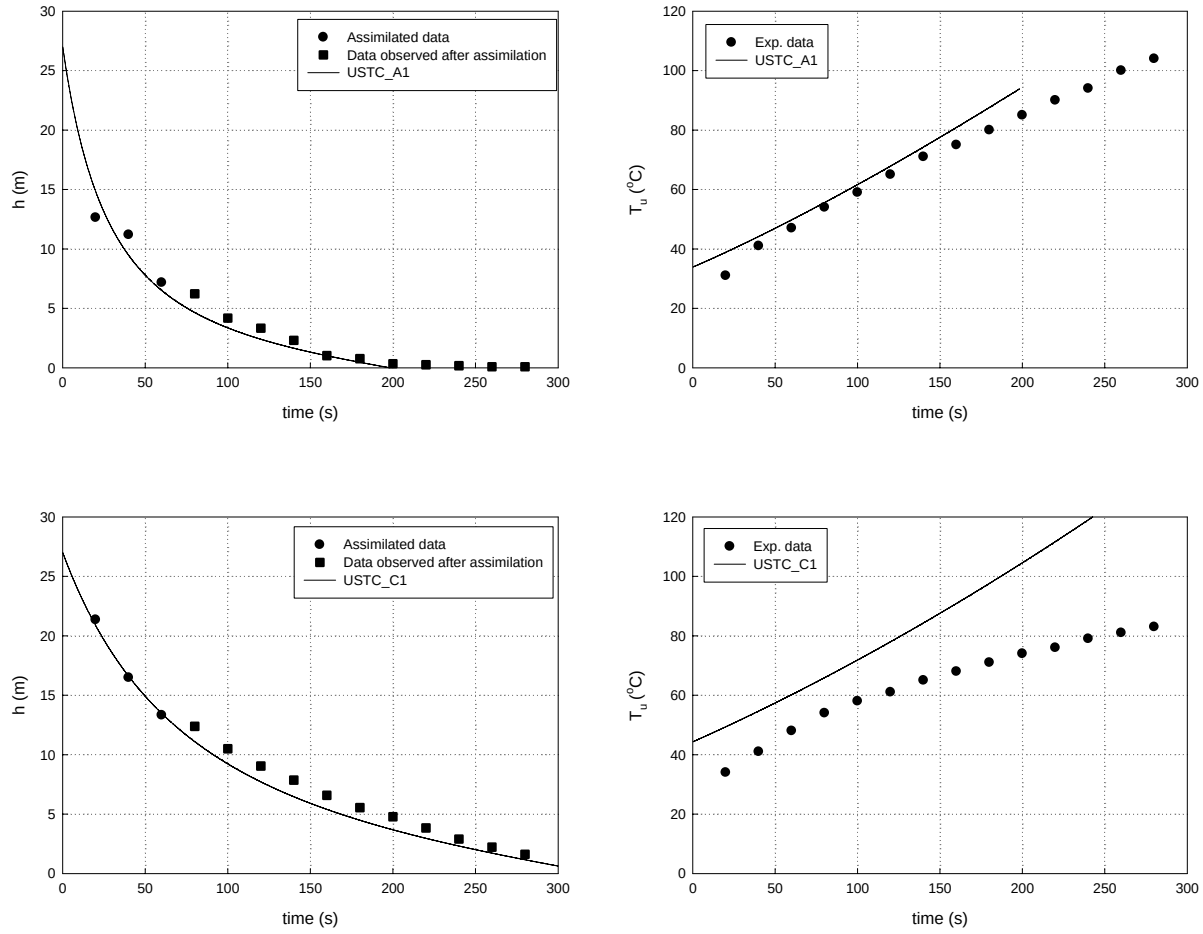

Figure 5. Evolution of smoke layer height (left) and temperature (right) for the fire in the middle (top) and in the corner (bottom) of the atrium floor. All symbols refer to experimental data, while lines correspond to simulation results. Only the first three measurements of smoke layer height have been assimilated; temperature data has not been assimilated, it is shown here only for comparison. Legend: see Table 3.

Data Assimilation for Smoke Layer Height and Temperature

If more than one variable is observed and assimilated, more accuracy can be expected in the forecasts. Table 4 provides an overview of the cases examined. The values are presented for the MIs after the optimization process when only 1 model parameter is kept constant. If *C* is chosen as MI, it is clear that, as in the previous section, the method automatically determines whether the

fire is in the middle of the atrium floor or not (compare USTC_A6 to USTC_C6 or USTC_A7 to USTC_C7). Therefore, it is recommended to use C as one of the MIs.

Table 4. Values obtained for MIs after the optimization process when only 1 model parameter is kept constant.

Case ID	Fire location	Constant	MIs	Assimilation window	Assimilated parameters
USTC_A5	Centre	C = 0.2	Q_c = 7293 kW α = 0.273	N=3, t ∈ [20s, 60s]	h and T_u
USTC_A6	Centre	α = 0.6	Q_c = 3323 kW C = 0.260	N=3, t ∈ [20s, 60s]	h and T_u
USTC_A7	Centre	Q_c = 4000 kW	C = 0.244 α = 0.500	N=3, t ∈ [20s, 60s]	h and T_u
USTC_C5	Corner	C = 0.1	Q_c = 3368 kW α = 0.468	N=3, t ∈ [20s, 60s]	h and T_u
USTC_C6	Corner	α = 0.6	Q_c = 2627 kW C = 0.109	N=3, t ∈ [20s, 60s]	h and T_u
USTC_C7	Corner	Q_c = 4000 kW	C = 0.094 α = 0.394	N=3, t ∈ [20s, 60s]	h and T_u

Figure 6 illustrates that differences between the forecasts are marginal (invisible). Comparison to Figure 5 reveals that the temperature predictions substantially improve when two MIs are used instead of only one, especially for the corner fire. This is confirmed by using Eq. (11). The latter gives a relative deviation in temperature of 44% with 1 MI and 6 % with 2 MIs.

However, it can be argued that the smoke layer height is a more important parameter than its temperature (since the temperatures are low). Therefore, the method, using only one MI, is considered to be reliable, i.e. not much accuracy is lost when the number of MIs is reduced from two to one. This makes the method attractive for use in practice, where DA can often be done for only one parameter.

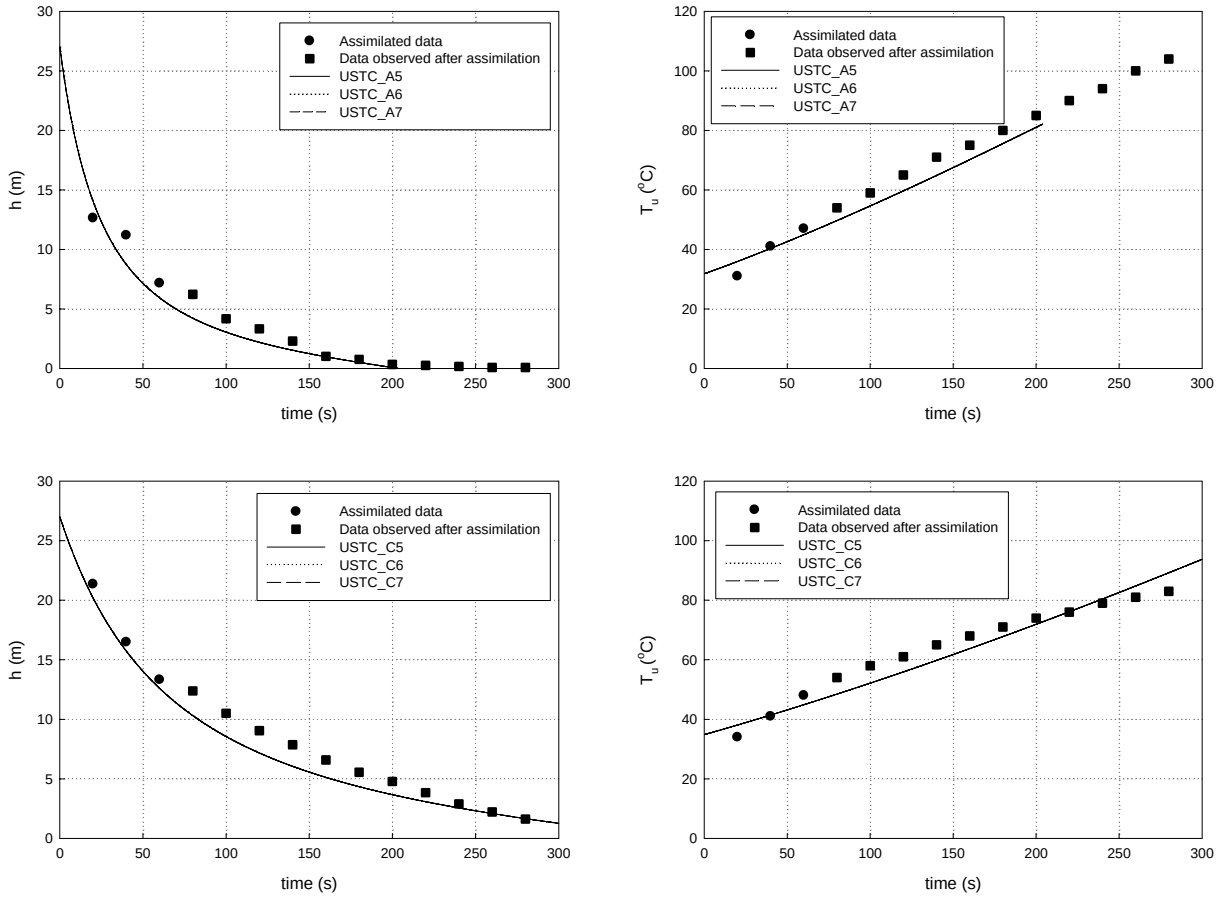

Figure 6. Evolution of smoke layer height (left) and temperature (right) for the fire in the middle (top) and in the corner (bottom) of the atrium floor – Use of 2 MIs. All symbols refer to experimental data, while lines correspond to simulation results. Only the first three measurements of smoke layer height and temperature have been assimilated. Legend: see Table 4.

Initial Guess and Convergence

For cases USTC_A6 and USTC_C6, Figure 7 shows that, starting from different initial guesses for Q_c, convergence is obtained very quickly. Except for very low (or high) initial guesses, the end value is obtained after 4 iterations or less. This end value does not depend on the initial guess value.

Figure 8 shows the ranges of initial Q_c for which the method converges. The lower the initial guess for C, the wider the interval for initial guess of Q_c for which the method converges. Therefore, a low value is recommended for C as initial guess. For Q_c a value of e.g. 500kW can be recommended as initial guess for the case at hand. The range for initial guess of α is also very wide, [0.01, 1.00] (not shown). A value α = 0.6 or 0.7 could be recommended as initial guess, which is, in general, a reasonable estimate for the radiative fraction of a fire for most common fuels.

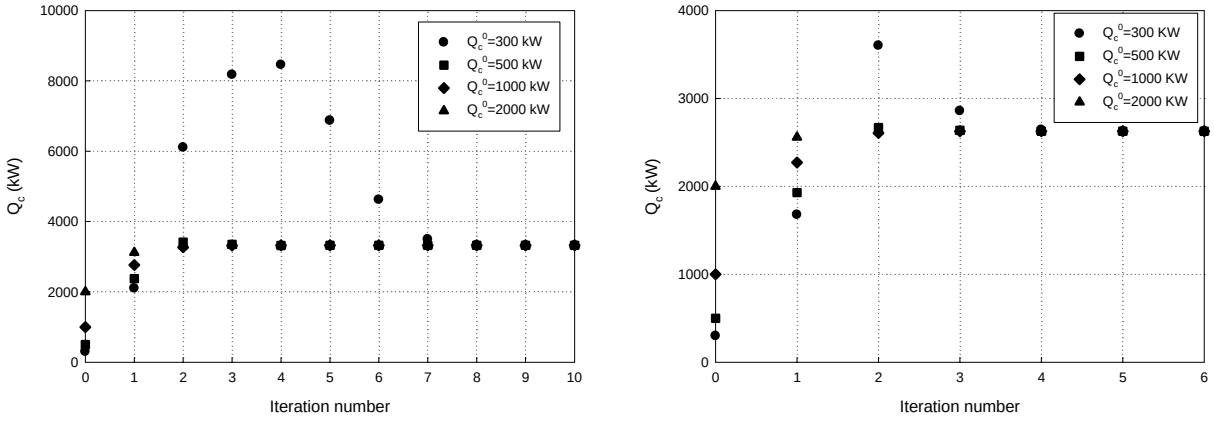

Figure 7. Convergence towards the optimized value of Q_c for USTC_A6 (C = 0.2) and USTC_C6 (C = 0.1).

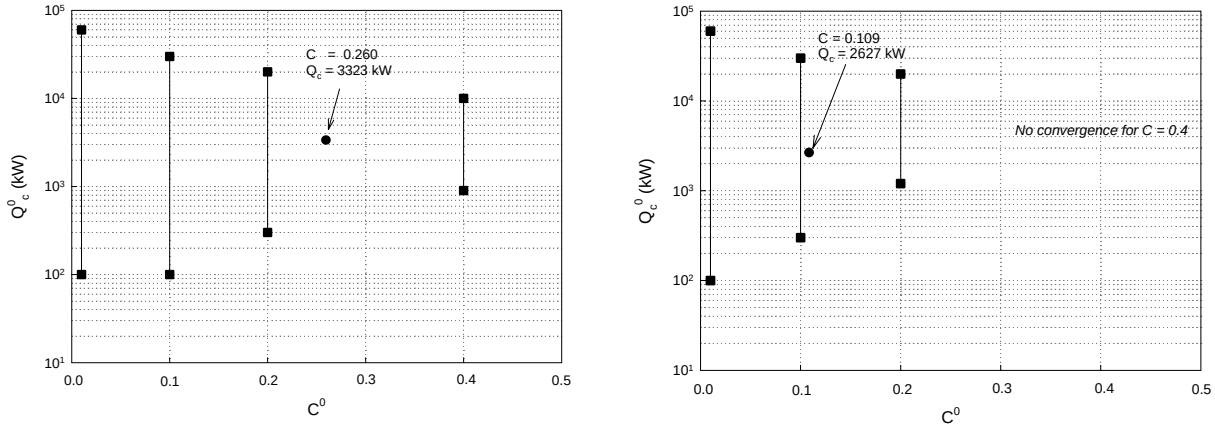

(a) (b)

Figure 8. Intervals of convergence for the initial guess of Q_c as a function of the initial guess of C for the cases USTC_A6 and USTC_C6.

Sensitivity of Results to DA Window

In this section we examine the effect of the assimilation window length and the positioning of the assimilation window on the time axis. Table 5 summarizes the results for the MIs.

Table 5. Effect of DA window on values for MIs.

Case ID	Assimilation window	Constant(s)	Optimized values of MIs
USTC_A6	$N = 3$, $t \in$ [20s, 60s]	$\alpha = 0.6$	$Q_c = 3323$ kW , $C = 0.260$
USTC_A6_1	$N = 2$, $t \in$ [20s, 40s]	$\alpha = 0.6$	$Q_c = 2903$ kW , $C = 0.273$
USTC_A6_2	$N = 4$, $t \in$ [20s, 80s]	$\alpha = 0.6$	$Q_c = 3583$ kW , $C = 0.252$
USTC_C6	$N = 3$, $t \in$ [20s, 60s]	$\alpha = 0.6$	$Q_c = 2627$ kW , $C = 0.109$
USTC_C6_1	$N = 2$, $t \in$ [20s, 40s]	$\alpha = 0.6$	$Q_c = 2189$ kW , $C = 0.107$
USTC_C6_2	$N = 4$, $t \in$ [20s, 80s]	$\alpha = 0.6$	$Q_c = 2846$ kW , $C = 0.106$
USTC_C6_3	$N = 3$, $t \in$ [80s, 120s]	$\alpha = 0.6$	$Q_c = 2730$ kW , $C = 0.080$

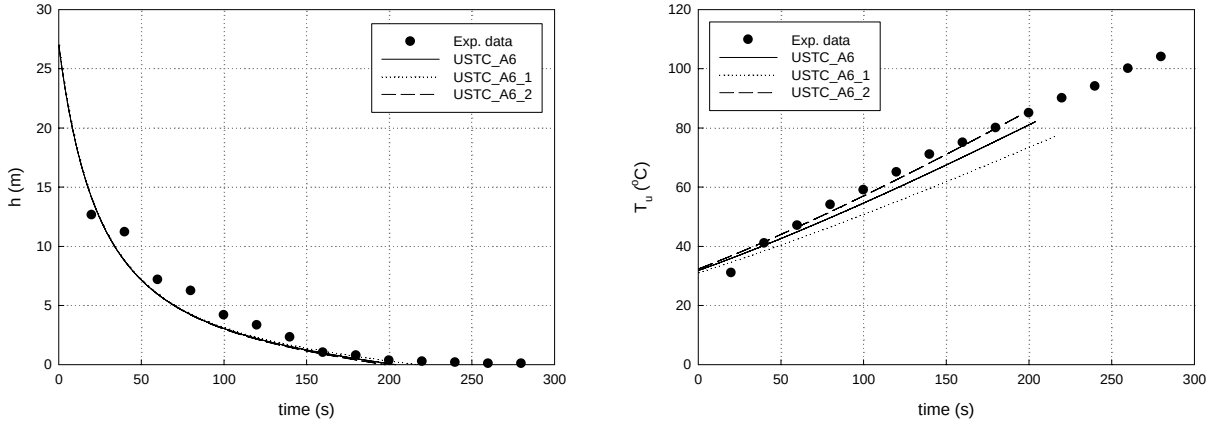

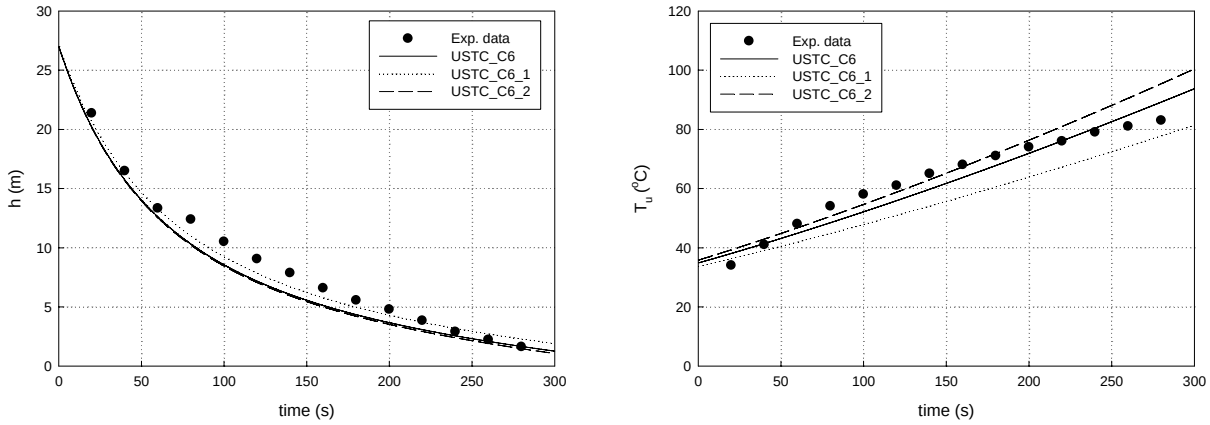

Figure 9. Effect of the DA window length for USTC_A6 (top) and USTC_C6 (bottom). Smoke layer height (left) and mean temperature (right). Legend: see Table 5.

Figure 9 shows that modifying the length of the DA window only, hardly affects the predictions for smoke layer height evolution (deviations in h are between 13 and 22 %). If 'quality' observations are provided over a given period of time, widening the assimilation window does not significantly improve the quality of the forecast for the smoke layer height. This is in line with the conclusion by Jahn et al. [9] who suggested the existence of an 'optimal assimilation window width'. The temperature predictions (which are, however, as explained above, less important), improve as the DA window widens, especially for the case USTC_A6.

One could also consider keeping the same DA window length, but moving it in time. The idea is then to replace 'old' information by more recent observations to improve the forecast. Figure 10 shows that indeed the forecast changes with the second assimilation window (*i.e.* N = 3, $t \in$ [80s, 120s]). Table 5 shows a decrease by 26.61 % in the optimized value of C from 0.109 for case USTC_C2 to 0.080 for USTC_C2_3. The change in the optimized value of Q_c is not significant.

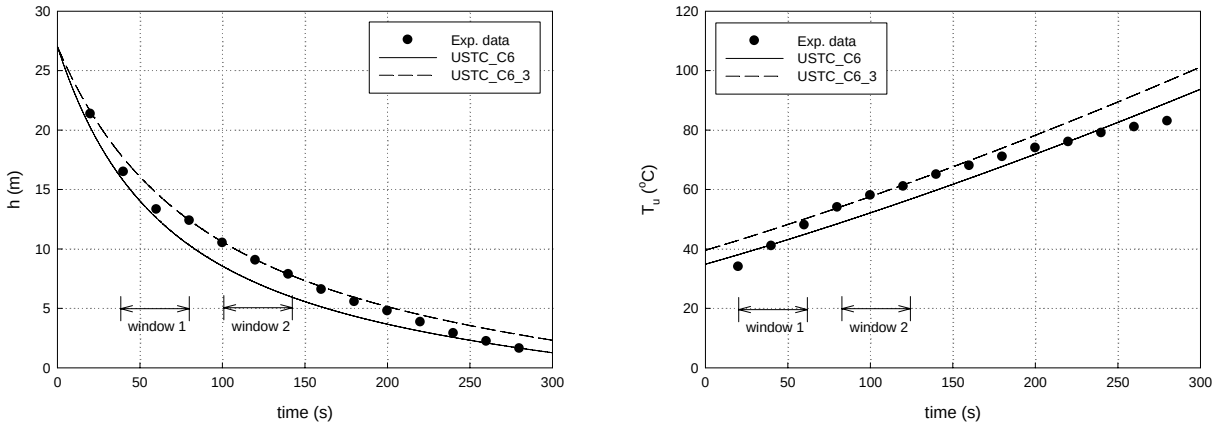

Figure 10. Effect of the DA window position for USTC_C6. Smoke layer height (left) and mean temperature (right). Legend: see Table 5.

CONCLUSIONS

The concept of numerical fire forecasting using live data from sensor readings has been applied to the case of natural smoke filling of a large atrium in case of fire.

The method of determining the values for the model invariant(s) (MI(s)) from the data assimilation (DA) for the observed variables has been explained.

Accurate forecasting of the smoke layer height evolution has been illustrated, with positive lead times of several minutes. This has been achieved by assimilating observations of smoke layer height over 60 s. Moreover, a simple expression for the smoke plume mass flow rate has been used. Due to the automatic adjustment of the entrainment coefficient, taking advantage of the DA process, the simple expression provides a sufficient level of quality. Another advantage of using the entrainment coefficient as MI, is the automatic 'determination' of the fire location. Indeed, the strong difference in entrainment between a plume originating from the middle of the floor as compared to a plume originating from a corner, is automatically reflected in a much

higher value for the entrainment coefficient in the former case. Therefore, it is recommended to use the entrainment coefficient as MI.

Forecasts for the smoke layer temperature improve substantially when 2 MIs are used, instead of 1, and DA is also performed for the smoke layer temperature. Since often the smoke layer height is more important than its temperature for the case at hand, the method is considered sufficiently accurate, using only 1 MI.

The method has been illustrated to be very robust with respect to the initial guess for the MI(s) and rapid convergence to the same values is obtained, independent of the initial guess. Making the DA window longer did not lead to a substantial improvement in the accuracy of the forecasts. Shifting the DA window in time does modify the results. This is a relevant feature for a dynamic DA procedure, but this is considered beyond the scope of the present paper.

ACKNOWLEDGEMENTS

This research has been funded by the Fund of Scientific Research – Flanders (Belgium) (FWO-Vlaanderen) through project G.0060.09.

NOMENCLATURE

A intermediate calculation matrix

A_{atrium} atrium floor area (m^2)

C variable plume entrainment coefficient

C_m constant plume entrainment coefficient (C_m = 0.21, Eq. (16))

C_p gas specific heat (=1 kJ/kg.K)

E energy (kJ)

H_0 ceiling height (m)

H_i intermediate calculation matrix

J cost function (m^2)

M_i output matrix of the forward model

N number of observations

Q_c convective heat release rate (kW)

T temperature (K)

V volume (m^3)

W_i weight matrix (taken as Identity)

b intermediate calculation matrix

g gravitational acceleration (=9.81 m/s^2)

h smoke layer height (m)

k_{LF} fire location factor (see Eq. (16))

$\dot{m}$ mass flux (kg/s)

t time (s)

y_i vector of observations or calculated values

z elevation above the fire (m)

Δt time step (s)

α heat coefficient taking into account radiative losses

ε relative deviation between experiments and predictions

θ vector of model invariants

ρ density (kg/m^3)

Subscripts

a ambient conditions

p plume

u upper layer

Superscripts

ˆ observation data

' perturbed value

T transpose matrix

REFERENCES

[1] Welch S., Usmani A., Upadhyay R., Berry D., Potter S., Torero J. and Rein G. (2007). Introduction to FireGrid, In: Abecassis C and Carvel R, editors. The Dalmarnock fire tests: experiments and modeling, The University of Edinburgh, 7-29.

[2] Cowlard A., Jahn W., Abecassis-Empis C. and Rein G. (2010). Sensor Assisted Fire Fighting, Fire Technol., 46: 719-741.

[3] Verstockt S., Van Hoecke S., Tilley N., Merci B., Sette B., Lambert P., Hollemeersch C. and Van de Walle R. (2011). FireCube: a multi-view localization framework for 3D fire analysis, Fire Safety J., 46: 262-275.

[4] Verstockt S., Merci B., Sette B., Lambert P. and Van de Walle R. (2010). Hot topics in video fire analysis, Newsletter of the International Association of Fire Safety Science (IAFSS), 29:14-15.

[5] Verstockt S., Vanoosthuyse A., Van Hoeke S., Lambert P. and Van de Walle R. (2010). Multi-sensor fire detection by fusing visual and non-visual flame features, Lecture Notes in Computer Science, 6134: 333-41.

[6] Calderara S., Piccinini P. and Cucchiara R. (2010). Vision based smoke detection system using image energy and color information, Mach. Vision Appl., 1–15.

[7] Owrutsky J.C., Steinhurst D.A., Minor C.P., Rose- Pehrsson S.L., Williams F.W. and Gottuk D.T. (2006). Long Wavelength Video Detection of Fire in Ship Compartments, Fire Safety J., 41:315-320.

[8] Günay O., Taşdemir K., Tőreyin B.U. and Cetin A.E. (2009). Video based wildfire detection at night, Fire Safety J., 44:860-868.

[9] Jahn W., Rein G. and Torero J.L. (2010). Forecasting fire growth using an inverse zone modeling approach, Fire Safety J., 46:81-88.

[10] Jahn W. (2010). Inverse Modelling to Forecast Enclosure Fire Dynamics, PhD thesis, The University of Edinburgh.

[11] Bouttier F. and Coutier P. (2001). Data assimilation concepts and methods, Technical Report, European Centre for Medium-Range Weather Forecasts.

[12] Korn P. (2009) Data Assimilation for the Navier-Stokes-α equations. Physica D, 238:1957-1974.

[13] Li Y.Z., Huo R., Yuan L.M., Li P.D., Fan W.C. and Cui E. (1999) Study of smoke filling processes in atrium, Journal of China University of Science and Technology, 29:590-4.

[14] Qin T.X., Guo Y.C., Chan C.K. and Lin WY. (2009) Numerical simulation of the spread of smoke in an atrium under fire scenario, Build. Environ., 44: 56-65.

[15] Zukoski E.E., Kubota T. and Cetegen B. (1981) Entrainment in Fire Plumes, Fire Safety J., 3:107-21.

[16] Heskestad G. (2002). Fire plumes, flame height and air entrainment, in: SFPE Handbook of Fire Protection Engineering (third ed.), NFPA, 2-1–2-17.

[17] McCaffrey B.J. (1983). Momentum implications for buoyant diffusion flames, Combust. Flame, 52: 149–167.

[18] Leblanc M. and Trouvé A. (2009) Inverse modeling of enclosure fire dynamics, in: Proceedings of the 6th U.S. National Combustion Meeting.

[19] Kleespies T.J. Tangent Linear and Adjoint Coding. Short Course. *http://cimss.ssec.wisc.edu/itwg/groups/rtwg/tl_ad_lectures/TL_Lectures.pdf*

[20] Milke J.A. (1990). Smoke Management for Covered Malls and Atria, Fire Technol. 26:223-43.